

## Clay minerals as selective and shape-selective sorbents

R.M. Barrer

Chemistry Department, Imperial College, London, SW7 2AZ, England

**Abstract** - An account has been given of four modes of sorption based on clay minerals and their cation exchanged and pillared forms. Sorption of non-polar molecules on outgassed layer structures containing only inorganic interlayer cations such as  $\text{Na}^+$  or  $\text{Ca}^{2+}$  is confined to external surfaces only. This is also the case with the fibrous clays or palygorskites. Polar molecules penetrate the interlayer region of the layer structures, but only after a threshold pressure is exceeded. The thermodynamic basis of this behaviour has been given. When the interlayer space is completely filled by long chain organic cations, as in dimethyldioctadecylammonium montmorillonite, imbibition with swelling can occur to an extent governed by the cohesive energy density of the sorbate relative to that of the interlayer region. Selectivity can be specific for aromatics and heterocycles. Finally, after exchange with organic cations or with inorganic oxy-cations which permanently expand the interlayer region but do not fill all the space, a diverse range of microporous sorbents can be produced which possess many zeolite properties such as shape-selective sorption. Some aspects of these sorbents are discussed.

### 1. INTRODUCTION

Clay minerals increasingly attract attention as sorbents and catalysts. The fibrous clays or palygorskites are channel structures in which siliceous strips occur. A given strip is linked through shared edges to each of four other identical strips, two above and two below. (ref. 1). The cross-section normal to the strip lengths resembles a brick wall with each alternate brick removed and the resultant channels run parallel with the strips. Other clay minerals are layer structures. Where these layers carry a negative charge there are interlayer cations electrochemically equivalent to the anionic charge (smectites, vermiculites, micas).

The bonding between siliceous layers is not covalent, but involves electrostatic forces, dispersion forces and sometimes hydrogen bonding. Because of this layer silicates can expand to intercalate guest molecules to an extent not observed among zeolite sorbents. Weiss (ref. 2) has recorded the swelling in distilled water of a number of layer silicates having the triple layers found in mica, with results shown for Na- and Ca- forms in Table 1. Margarite mica with the highest layer charge and pyrophyllite and talc with zero layer charge did not swell, and thus did not intercalate water. For all the others the extent of swelling was sensitive both to the anionic layer charge and to the type of interlayer cation.

In this account I shall report four kinds of sorbent behaviour we have observed for smectites and vermiculites which can sometimes result in high selectivities including molecule sieving.

### 2. NON-POLAR SORBATES AND INORGANIC INTERLAYER CATIONS

When the interlayer cations were small inorganic ions like  $\text{Na}^+$  or  $\text{Ca}^{2+}$  well outgassed smectites and vermiculites did not intercalate non-polar molecules such as n-, iso-, neo- and cyclo-paraffins or benzene or toluene (ref. 3). Likewise these non-polar molecules did not enter the channels present in the palygorskites (ref. 4). The sorption isotherms on the external surfaces were of type 2 in Brunauer's classification (ref. 5). At relative pressures where multilayers and capillary condensate occur there are hysteresis loops which close at relative pressures in the range 0.27 to 0.47, according to the sorbate and the temperature. These features are displayed in Fig. 1. (ref. 3). From the isotherms the external monolayer equivalent areas can be determined. As shown in Table 2, for the clay minerals investigated in my laboratory, the external areas range from very limited to large, according to size and morphology of the crystals. The fibrous clays, attapulgite and sepiolite, are already high area sorbents, without involving intracrystalline sorption.

TABLE 1. The relation between swelling in distilled water and charge density of silicates having the triple layers found in micas (ref. 2).

Silicate	Interlayer surface per unit charge ( $\text{\AA}^2$ )	Extent of swelling in $\text{\AA}$ :	
		Na- form	Ca- form
Margarite	12	0	0
Muscovite	24	1.9	2.8
Biotite	24	1.9	2.8
Lepidolite	24	1.9	2.8
Zinnwaldite	24	1.9	2.8
Seladonite	27	2.4	2.8
Glauconite	31	3.8	2.8
Diocahedral illite	32	4.2	2.8
Triocahedral illite	36	5.1	4.3
Vermiculite	36	5.1	4.3
Vermiculite	36	5.0	4.2
Vermiculite	37	5.1	4.2
Batavite	36	5.1	4.3
Beidellite I	41	5.4	4.9
Saponite	42	4.9	4.9
Nontronite	46	$\infty$	9.2
Beidellite II	57	$\infty$	9.2
Montmorillonite	60	$\infty$	9.2
Montmorillonite	75	$\infty$	9.6
Hectorite	100	$\infty$	10.6
Pyrophyllite	$\infty$	0	0
Talc	$\infty$	0	0

TABLE 2. External surface areas,  $A_e$ , of some clay minerals

Clay Mineral	c.e.c. in meq/100g*		$A_e/m^2g^{-1}$
Fluorhectorite <sup>0</sup>	150	8	
Fluorhectorite <sup>0</sup>	90	11	
Bentone 34 (dimethyldioctadecylammoniummontmorillonite)	-	14.8	
Montmorillonite (Na-rich)	91	21.7	
Hectorite (Ben-a-Gel)	90	81.4	
Montmorillonite (Ca-rich)	102	85.4	
Attagulgite	-	195 (max.)	
Sepiolite	-	235 (max.)	

\* c.e.c. = cation exchange capacity; meq = milliequivalents  
0 = Synthetic

For n-, iso- and neo-pentane, outgassing the attapulgitite at each of a series of progressively increasing temperatures produced the correlated changes between rate of water loss, surface area, BET affinity constants and uptakes at relative pressure of 0.1 which are shown in Fig. 2 (ref. 4). For attapulgitite outgassed below 100°C there was a selectivity sequence



but after outgassing above 100°C, as the probable result of structural changes in the sorbent (ref. 7), this selectivity almost disappeared.

Because adsorption on external surfaces will always occur one must allow for this when evaluating amounts intercalated and available interlayer areas.

### 3. POLAR SORBATES AND INORGANIC INTERLAYER CATIONS

In well outgassed smectites and vermiculites, in which the interlayer cations were again small ions such as  $\text{Na}^+$  and  $\text{Ca}^{2+}$ , sorption was initially limited to external surfaces. However, at approximate critical pressures which varied with sorbate, cation and temperature, intercalation of polar molecules began and resulted in one or two steps in the isotherms (ref. 3). These steps are illustrated in Fig. 3 (ref. 8) for pyridine and water in the Na-rich montmorillonite of Table 2. A second feature was hysteresis between sorption and desorption branches of the isotherms which persisted to very low pressures. Both these features require explanation.

### 4. THE CONDITION FOR INTERCALATION THRESHOLDS

An interpretation of and requirement for intercalation threshold pressures has been given (ref. 8). The unexpanded, outgassed parent clay mineral will be termed the  $\alpha$ -phase and the expanded phase after intercalation the  $\beta$ -phase. For uptake of  $n$  moles of guest,  $M$ , we may write the equation



the free energy change for which is  $\Delta G$  under the experimental conditions of temperature and pressure.  $\Delta G$  has two components. The first is a positive term,  $\Delta G_{\alpha\beta}$ , which is the free

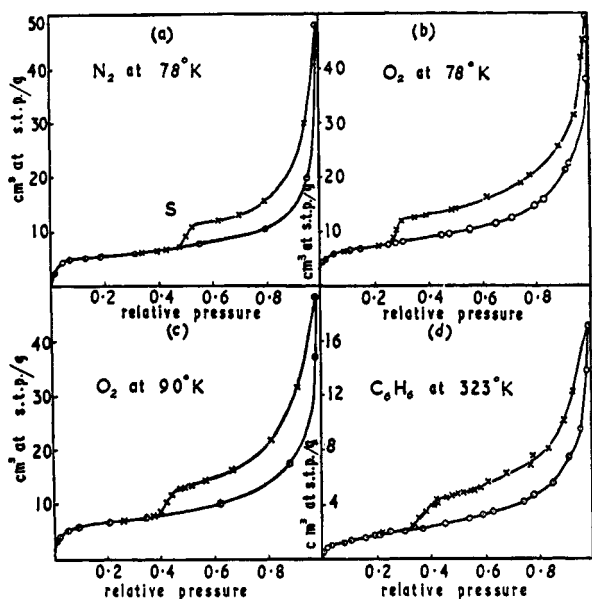


Fig. 1. Isotherms typical of layer silicate (here a Na-rich montmorillonite) behaving as a non-permeable sorbent (ref. 3). S indicates the characteristic shoulder at the closure of the hysteresis loop. O = sorption points; x = desorption points.

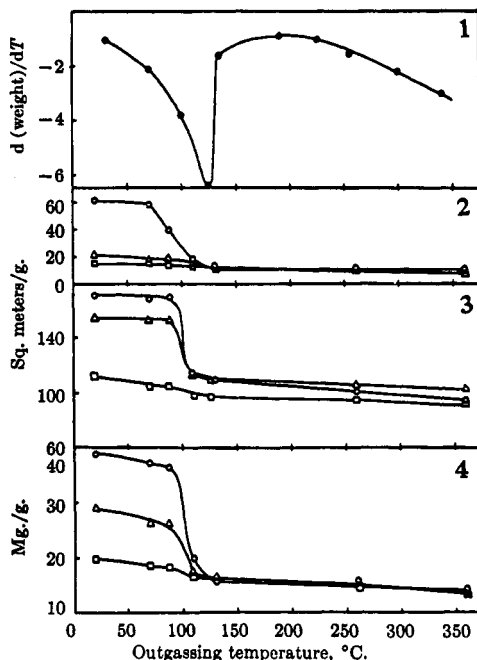


Fig. 2. Correlations between various aspects of sorption of isomeric pentanes on attapulgite and the outgassing temperatures (ref. 6) :

1. Rate of water loss from the attapulgite.
  2. The coefficient  $c$  in the BET isotherm.
  3. The areas available to the isomers.
  4. The uptakes at a relative pressure of 0.1.
- O,  $n\text{-C}_5\text{H}_{12}$ ;  $\Delta$ ,  $\text{iso-C}_5\text{H}_{12}$ ;  $\square$ ,  $\text{neo-C}_5\text{H}_{12}$ .

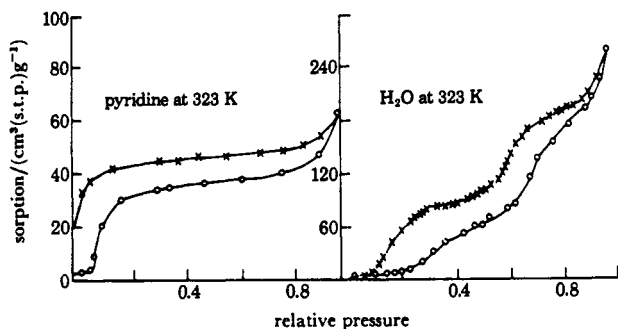


Fig. 3. Sorption of pyridine and water in Na-rich montmorillonite, showing threshold pressures, isotherm steps and hysteresis persisting to low relative pressures (ref. 3 and 8).

energy change on expanding the  $\alpha$ -phase to the sorbate free  $\beta$ -phase. The second, which is negative, is the free energy change,  $\Delta G_1$ , when the  $n$  moles of guest enter the  $\beta$ -phase. Thus

$$\Delta G = \Delta G_{\alpha\beta} + \Delta G_1 \tag{2}$$

and whether intercalation can proceed or not will depend on the relative magnitudes of  $\Delta G_{\alpha\beta}$  and  $\Delta G_1$ . For  $\Delta G$  positive, intercalation is not expected; for  $\Delta G$  negative, intercalation can occur.

The  $\beta$ -phase intercalates are a type of solid solution of guest in host to which we now apply the Gibbs-Duhem relation at constant temperature:

$$n_\beta d\mu_\beta + nd\mu_M = Vdp \tag{3}$$

Here  $n_\beta$  denotes the number of moles of the host comprising the  $\beta$ -phase. A convenient measure of this mole could be the guest-free gramme unit cell content.  $\mu_\beta$  and  $\mu_M$  are the chemical potentials of host and guest in the solution of volume  $V$  at pressure  $p$  (normally the vapour pressure of the guest at equilibrium with the solution). Also  $d\mu_M = RT \ln a$  where  $a$  denotes the activity of the guest. We can re-arrange eqn. 3 and integrate between  $a = 0$  and

a, the result being

$$\mu_{\beta} = \mu_{\beta}^{\ominus} + pV_{\beta} - RT \frac{n_{\text{sat}}}{n_{\beta}} \int_0^{\theta} \frac{\theta}{a} da \quad (4)$$

in this expression  $\mu_{\beta}^{\ominus} = G_{\beta}^{\ominus}$  is the free energy of a mole of pure (i.e. guest-free)  $\beta$ -phase.  $V = V/n_{\beta}$  is the molar volume of the  $\beta$ -phase, which is a constant because the  $\beta$ -phase is already fully expanded and so does not expand further when accommodating the guest. In eqn. 4  $n$  has been replaced by  $n_{\text{sat}} \theta$  where  $n_{\text{sat}}$  is the saturation uptake of guest inside the  $\beta$ -phase and  $\theta$  is the degree of saturation for an uptake of  $n$  moles of guest.

As  $\theta$  in eqn. 4 increases so  $\mu_{\beta}$  must decrease. The free energy of reaction 1 is the difference in free energy of the host-guest solution and of the pure components, i.e.

$$\Delta G = n_{\beta} \mu_{\beta} + n_{\text{M}} \mu_{\text{M}} - (n_{\beta} \mu_{\alpha}^{\ominus} + n_{\text{M}} \mu_{\text{M}}^{\text{g}}) \quad (5)$$

where  $\mu_{\alpha}^{\ominus} = G_{\alpha}^{\ominus}$  is the free energy per mole of pure  $\alpha$ -phase and  $\mu_{\text{M}}^{\text{g}}$  the chemical potential of guest molecules in the gas phase. At intercalation equilibrium  $\mu_{\text{M}}^{\text{g}} = \mu_{\text{M}}$  so that eqns. 4 and 5 give

$$\Delta G_1 = \frac{\Delta G}{n_{\beta}} = (\mu_{\beta}^{\ominus} - \mu_{\alpha}^{\ominus}) + pV_{\beta} - RT \frac{n_{\text{sat}}}{n_{\beta}} \int_0^{\theta} \frac{\theta}{a} da \quad (6)$$

The critical condition for intercalation to commence arises when  $\Delta G_1 = 0$ , i.e. as  $\Delta G_1$  changes with increasing  $\theta$  from positive to negative. The critical condition is therefore

$$\mu_{\alpha}^{\ominus} - \mu_{\beta}^{\ominus} = V_{\beta} p - \frac{n_{\text{sat}}}{n_{\beta}} \int_0^{\theta} \frac{\theta}{a} da \quad (7)$$

The integral can in principle be found from graphical integration of the isotherm plotted as  $e/p$  against  $p$ , since usually one can take  $p$  as a measure of activity. However, the isotherm for intercalation can be measured only in the pressure range above the critical or threshold pressure so that an extrapolation to zero pressure is required and uncertainty is thereby introduced in evaluating  $\Delta G_{\alpha\beta} = (\mu_{\alpha}^{\ominus} - \mu_{\beta}^{\ominus})$  from eqn. 7.  $V_{\beta} p$  is usually negligible.

The extent of swelling required for intercalation varies from one guest molecule to another (according to molecular size, shape and orientation of the guest between layers) as does the isotherm of the guest in the  $\beta$ -phase. Therefore there will be a different temperature dependent threshold pressure for each guest molecule in a given clay mineral. Also there will be a different threshold pressure for the same guest in each different clay mineral, because the work in separating the layers will differ according to layer charge and composition, and to the type of interlayer cation.

The foregoing analysis has wide generality: it is applicable to zeolite formation from other minerals in which the usual guest is water, and to clathration, both of which represent solid solutions of host plus guest. It is also applicable to intercalation in layer structures other than clay minerals, for example graphite and certain layer sulphides. Fig. 4. shows as an illustration, the isotherms we have obtained for clathration of Kr in phenol, above the threshold pressures (ref. 9).

When there is more than one step in the intercalation isotherm (e.g.,  $\text{H}_2\text{O}$  in Fig. 3), there is a second transition from  $\beta$ -phase intercalate to  $\gamma$ -phase intercalate.<sup>2</sup> The foregoing treatment then applies to this step with  $\alpha$  and  $\beta$  replaced throughout by  $\beta$  and  $\gamma$  respectively.

## 5. HYSTERESIS ASSOCIATED WITH INTERCALATION

We have also to account for the persistent hysteresis between the sorption and desorption branches shown in Fig. 3. The change of the crystal from its  $\alpha$ -phase to the guest-bearing  $\beta$ -phase involves nucleation at the periphery of the  $\alpha$ -phase. Nucleation involves two positive free energy terms: a strain free energy  $\Delta g_{\text{s}}$  and an interface free energy,  $\Delta g_{\sigma}$ . For a nucleus with  $j$  included guest molecules its free energy of formation is thus

$$\Delta g_j = \Delta G_2(j/N_A) + \Delta g_{\sigma} + \Delta g_{\text{s}} \quad (8)$$

rather than

$$\Delta g_j = \Delta G_2(j/N_A) \quad (9)$$

In these expressions  $\Delta G_2$  is the free energy of formation of the amount of  $\beta$ -phase intercalate containing one mole of the guest at the value of  $\theta$  corresponding with pressure  $p$  of the intercalation isotherm and  $N_A$  is Avogadro's number. At the true threshold pressure  $\Delta G_2$  is

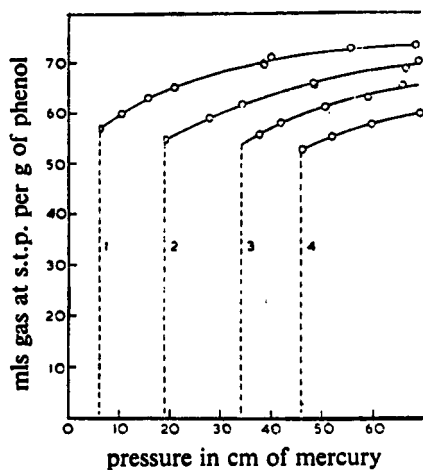


Fig. 4. Sorption isotherms of Kr in phenol above the threshold pressures (ref. 9.). (1) 195K; (2) 212K; (3) 222.2K; and (4) 228K.

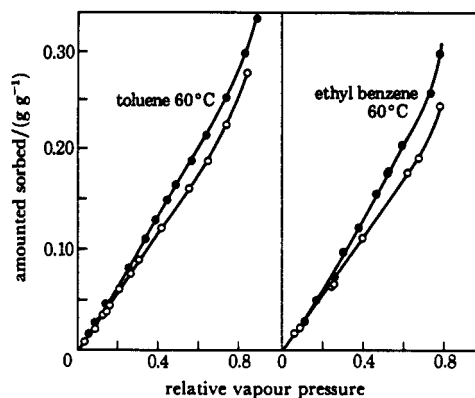


Fig. 5. Isotherms for toluene and ethylbenzene obtained with Bentone 34 (dimethyldioctadecylammonium montmorillonite) (refs. 10 and 8). o, sorption; ●, desorption

zero, as considered in the previous section, but  $\Delta g_i$  in eqn. 8 is still positive. Accordingly nucleation of  $\beta$ -phase intercalate is delayed to pressures above the true thermodynamic threshold pressure. For the same reason, on desorption, nucleation of the  $\alpha$ -phase will also be delayed to pressures below the true thermodynamic threshold. The result is the intercalation hysteresis which was seen in Fig. 3.

## 6. SORBATES IMBIBED BY ORGANO-CLAYS

The third kind of behaviour of sorbents obtained from clay minerals is exemplified by Bentone 34, (Table 2) which is a montmorillonite exchanged with dimethyldioctadecylammonium ions. The large organic cations fill all the space between siliceous layers and expand  $d(001)$  to 23.2Å. This sorbent imbibed some types of sorbate, notably aromatic hydrocarbons and heterocycles, but not others (ref. 10). Where imbibition was substantial the  $d(001)$  spacing expanded further, and the isotherms tended to be of type 3 in Brunauer's classification, as seen in Fig. 5 (ref. 8) for toluene and ethylbenzene. These isotherm contours recall the contours found when benzene is sorbed by cross-linked elastomers, and therefore suggest that imbibition may be controlled by the cohesive energy densities of the sorbates (C.E.D. = molar energy of vapourisation of liquid sorbate divided by the molar volume of the liquid). This view is supported by the results in Table 3.

For iso-octane and cyclo-hexane  $d(001)$  is the same, within experimental uncertainty, as that for the parent Bentone 34 and the small observed uptakes are therefore nearly all on the external surface. For toluene and benzene  $d(001)$  increased substantially and the uptake is largely by imbibition. The selectivity of imbibition for aromatics and heterocycles over paraffins and cyclo-paraffins is notable. The maximum imbibition should occur when the C.E.D. of the sorbate most closely matches that of the organic interlayer as modified by the presence of adjacent siliceous layers.

TABLE 3. Sorption by Bentone 34 at  $p/p_0 \approx 0.2$  related to C.E.D. and  $d(001)$  spacings (ref. 10)

Sorbate	$\left[ \frac{\text{C.E.D.}}{\text{cal/cm}^3} \right]^{1/2}$	$T^\circ \text{C}$	mmole sorbed per g at $T$ & $p/p_0 \approx 0.2$	$\frac{d(001)}{\text{Å}}$
iso-butane	6.25	-30	0.06 <sub>2</sub>	-
n-butane	6.7	-30	0.07 <sub>7</sub>	-
iso-octane	6.85	45	0.11 <sub>7</sub>	23.2
n-heptane	7.45	45	0.11	23.2
cyclo-hexane	8.20	45	0.16	23.2
ethylbenzene	8.8	60	0.52	-
toluene	8.90	45	0.65	27.2
benzene	9.15	45	0.81	27.2
dioxane	10.0	60	0.92	-
pyridine	10.7	60	1.79	-
nitromethane	12.6	45	1.38	-

Bentone 34 is just one member of a class of expanded but non-porous layer silicates in which all interlayer space is filled by large organic cations. Their selectivities deserve more investigation.

### 7. SORPTION IN PERMANENTLY MICROPOROUS LAYER SILICATES

The fourth type of behaviour is exhibited by layer silicates which have been made permanently microporous. About 1950 it seemed to me that if the small inorganic cations between the layers were replaced by larger ions such as  $\text{Me}_4\text{N}^+$  ( $\text{Me} = \text{CH}_3$ ) the siliceous layers would be held apart permanently, thus creating interlamellar micropores accessible to any molecules of the right shape and size to fit between the cations and the siliceous layers. This reasoning is shown schematically in Fig. 6 (ref. 11). It is the dimensions  $d_1$  and  $d_3$  which control access to the interlamellar pore spaces.

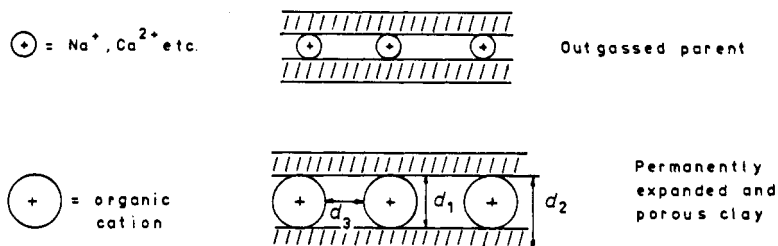


Fig. 6. Representation of the permanent expansion of a layer silicate by exchanging small interlayer cations for large ones (ref. 11).

The correctness of this surmise was shown in a paper of 1955 (ref. 12) in which the exchange ions were  $\text{Me}_4\text{N}^+$  and  $\text{Et}_4\text{N}^+$  ( $\text{Et} = \text{C}_2\text{H}_5$ ). The expanded clay minerals functioned as molecular sieves and freely intercalated many permanent gases and non-polar hydrocarbons which were not intercalated by the parent Na-montmorillonite. The sorption capacity was thereby greatly increased. This work was developed further over subsequent years using several different types of layer silicate and a variety of organic cations and also  $\text{Co}(\text{en})_3^{2+}$ , where "en" denotes ethylenediamine. It revealed many interesting selective and shape-selective separation capabilities.

Inclusion isotherms (derived from the total uptakes corrected for sorption upon external surfaces) are of type 1 in Brunauer's classification (ref. 5) and so recall those normally observed in zeolite sorbents. This is seen in Fig. 7 (ref. 13) for  $\text{N}_2$  and Ar at 78K in a series of alkylammonium and alkylidiammonium montmorillonites and hectorites. The

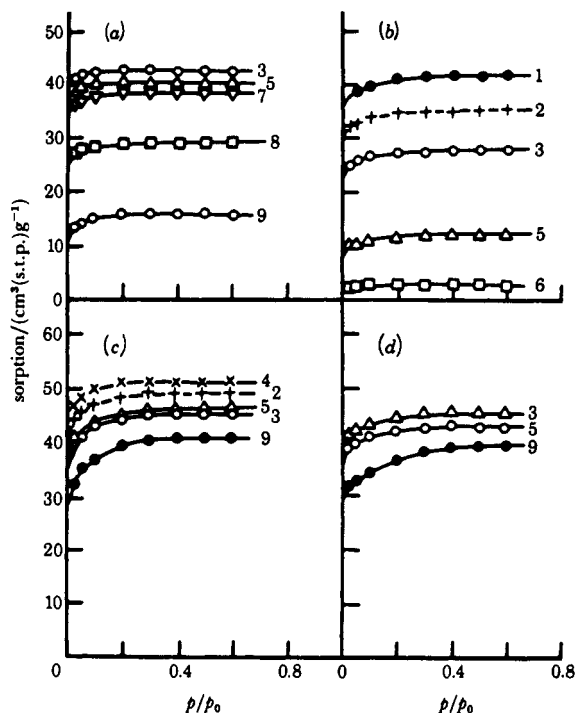


Fig. 7. Interlamellar parts of the sorption isotherms for  $\text{N}_2$  and Ar at 78K (refs. 13 and 8)

- (a)  $\text{N}_2$  in alkylidiammonium montmorillonites.
- (b)  $\text{N}_2$  in alkylammonium montmorillonites.
- (c)  $\text{N}_2$  in alkylidiammonium hectorites.
- (d) Ar in alkylidiammonium hectorites.

The numbers by the curves are the carbon numbers of the organic cations.

saturation interlayer uptakes decline with increasing chain length. Saturation capacities are greater, and the decline with carbon number of the cation is less marked, for alkyldiammonium than for alkylammonium ions. This is expected because the total number of divalent exchange ions is only half the number of monovalent ones.

Permanent intracrystalline pore volumes were estimated for the sorbate-free layer silicates from the total interlayer areas less the areas covered by the cations, multiplied by the measured free distances,  $d_1$  in Fig. 6, between adjacent siliceous layers. Table 4 (ref. 13) shows the considerable total micropore volumes.

The free distance,  $d_1$ , between the sheets of the expanded clay mineral is not necessarily fixed, but may expand further to intercalate appropriate guest molecules (see below). Total micropore volumes of the guest-bearing layer silicates were therefore also evaluated for two  $\text{Co}^{\text{III}}(\text{en})_2$ -fluorhectorites with c.e.c.'s of 90 and 150 meq per 100g, respectively termed FH90 and FH150. The pore volumes in Table 5 (ref. 15) are given as  $\text{cm}^3$  of liquid sorbate intercalated per g, of sorbent at saturation of the interlayer pore volume.

The behaviour of these permanently porous layer silicates can be considered in terms of eqn. 2 ( $\Delta G = \Delta G_{\alpha\beta} + \Delta G_i$ ). If  $d_1$  and  $d_3$  are sufficient for the guest to be intercalated without further increase in  $d_1$ , then  $\Delta G_{\alpha\beta}$  will be zero, so that  $\Delta G = \Delta G_i$  and therefore is always negative. No threshold pressure is then required for intercalation and so the isotherm is continuous, as is normal for a zeolite sorbent.

TABLE 4. Calculated interlayer free areas and porosities of some organo-montmorillonites and hectorites (ref. 13)

Cation	g.u.c. wt.	Ion co-area $\frac{\text{Å}^2}{\text{Å}}$	$\frac{d_1}{\text{Å}}$	Free area $\frac{\text{m}^2}{\text{g}^{-1}}$	Porosity $\frac{\text{cm}^3}{\text{g}^{-1}}$
(a) Alkylammonium montmorillonites (c.e.c. 85 meq/100g)					
$\text{CH}_3\text{NH}_3^+$	746	21.6	2.2	294	0.065
$\text{C}_2\text{H}_5\text{NH}_3^+$	755	29.8	3.4	214	0.073
$\text{C}_3\text{H}_7\text{NH}_3^+$	765	35.6	3.7	184	0.068
$n\text{-C}_4\text{H}_9\text{NH}_3^+$	774	41.4	3.9	155	0.060
$n\text{-C}_5\text{H}_{11}\text{NH}_3^+$	783	47.1	4.0	126	0.050
$n\text{-C}_6\text{H}_{13}\text{NH}_3^+$	792	52.9	4.0	98	0.039
(b) $\alpha$ , $\omega$ -alkyldiammonium montmorillonites (c.e.c. 85 meq/100g)					
$^+\text{NH}_3(\text{CH}_2)_2\text{NH}_3^+$	746	34.8	2.8	278	0.078
$^+\text{NH}_3(\text{CH}_2)_3\text{NH}_3^+$	750	40.6	3.5	262	0.092
$^+\text{NH}_3(\text{CH}_2)_4\text{NH}_3^+$	755	46.4	4.0	246	0.098
$^+\text{NH}_3(\text{CH}_2)_5\text{NH}_3^+$	759	52.2	3.9	231	0.090
$^+\text{NH}_3(\text{CH}_2)_6\text{NH}_3^+$	764	58.0	3.8	216	0.082
$^+\text{NH}_3(\text{CH}_2)_7\text{NH}_3^+$	769	63.7	3.9	201	0.078
$^+\text{NH}_3(\text{CH}_2)_8\text{NH}_3^+$	773	69.5	3.9	187	0.073
$^+\text{NH}_3(\text{CH}_2)_9\text{NH}_3^+$	778	75.3	3.9	172	0.067
(c) $\alpha$ , $\omega$ -alkyldiammonium hectorites (c.e.c. 91 meq/100g)					
$^+\text{NH}_3(\text{CH}_2)_2\text{NH}_3^+$	769	34.8	2.8	240	0.067
$^+\text{NH}_3(\text{CH}_2)_3\text{NH}_3^+$	774	40.6	3.6	224	0.080
$^+\text{NH}_3(\text{CH}_2)_4\text{NH}_3^+$	779	46.4	[3.9]	208	[0.081]
$^+\text{NH}_3(\text{CH}_2)_5\text{NH}_3^+$	783	52.2	3.9	192	0.075
$^+\text{NH}_3(\text{CH}_2)_9\text{NH}_3^+$	802	75.3	3.9	128	0.050

TABLE 5. Pore volumes in  $\text{Co}^{\text{III}}(\text{en})_3\text{-FH90}$  and  $\text{Co}^{\text{III}}(\text{en})_3\text{-FH150}$  estimated from monolayer saturation uptakes,  $\bar{v}_m$  (ref. 15)

Sorbate	$T$ K	$\bar{v}_m$ $\text{cm}^3$ at stp $\text{g}^{-1}$	Mol. Vol. at T $\text{cm}^3$	$\text{cm}^3$ (liq) per g. of sorbent
(a) $\text{Co}^{\text{III}}(\text{en})_3\text{-FH90}$				
$\text{O}_2$	77.3	67.8	26.5	0.08 <sub>0</sub>
$\text{O}_2$	90.2	66.5	27.9	0.08 <sub>3</sub>
$\text{N}_2$	77.3	51.3	34.7	0.07 <sub>9</sub>
$\text{N}_2$	90.2	45.7	37.4	0.07 <sub>6</sub>
Ar	77.3	65.6	27.4	0.08 <sub>0</sub>
Ar	90.2	63.7	29.1	0.08 <sub>3</sub>
$\text{CH}_4$	90.2	50.0	38.7	0.08 <sub>2</sub>
iso- $\text{C}_4\text{H}_{10}$	273.2	19.0	100.1	0.08 <sub>6</sub>
neo- $\text{C}_4\text{H}_{10}$	273.2	23.7	117.4	0.12 <sub>6</sub>
$\text{CO}_2$	273.2	31.4	47.4	0.06 <sub>4</sub>
(b) $\text{Co}^{\text{III}}(\text{en})_3\text{-FH150}$				
$\text{O}_2$	77.3	51.7	26.5	0.06 <sub>1</sub>
$\text{O}_2$	90.2	49.3	27.9	0.06 <sub>1</sub>
$\text{CO}_2$	273.2	21.4	47.4	0.04 <sub>5</sub>

Sometimes intercalation further increases  $d_1$ . In this case  $\Delta G_{\alpha\beta}$  is not zero. As examples one may consider methylammonium and tetramethyl ammonium montmorillonites in sorption equilibrium with n-heptane and benzene :

Exchange form	$d_1/\text{\AA}$	$d_1/\text{\AA}(\text{n-heptane})$	$d_1/\text{\AA}(\text{benzene})$
$\text{MeNH}_3^+$	2.2	3.6	5.6
$\text{Me}_4\text{N}^+$	4.1	4.1	5.2

In the  $\text{MeNH}_3$ -form the increase in  $d_1$  was particularly large for benzene intercalation and made  $\Delta G_{\alpha\beta}$  big enough for intercalation to require a low threshold pressure (ref. 16). This meant that when benzene and n-heptane were sorbed from their mixtures n-heptane was initially preferred. In contrast in the sorption of n-heptane/benzene mixtures by the  $\text{Me}_4\text{N}$ -form, the benzene was always preferred. Fig. 8 (ref. 17) then gives the fractionation factors for

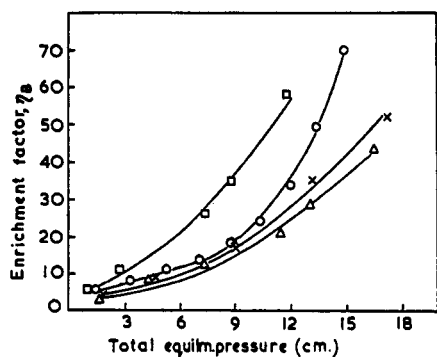


Fig. 8. Enrichment factors of benzene,  $\eta_B$ , as functions of temperature and total equilibrium pressure for a benzene-heptane mixture. The sorbent was  $(\text{CH}_3)_4\text{N}$ -montmorillonite and the feed mixture contained 0.67 mole fraction of benzene.

□, 80°C; ○, 85°C; ×, 90°C; △, 95°C.

benzene at several temperatures as a function of total pressure. This factor,  $\eta_B$ , is defined as

$$\eta_B = \frac{n_B^s p_H^g}{n_H^s p_B^g} \quad (10)$$

The  $n$  denote moles and the  $p$  are partial pressures. Subscripts B and H denote benzene and n-heptane and superscripts s and g denote sorbed and gaseous, respectively.



When one component was not intercalated and the other was (eg. cyclohexane and benzene in  $\text{MeNH}_3^-$ -montmorillonite) the separation factor was even greater. Many mixtures were well separated using shape-selective microporous clay mineral sorbents, as exemplified for the following pairs, using  $\text{Me}_4\text{N}$ -montmorillonite at 77°C (ref. 18) :

benzene/cyclohexane	cyclohexane/cyclohexanol
toluene/cyclohexane	n-heptane/methanol
benzene/n-heptane	n-hexane/cyclohexane
benzene/carbon tetrachloride	n-heptane/iso-octane
benzene/toluene	n-heptane/cyclohexane
methanol/carbon tetrachloride	thiophene/benzene

## 8. TAILORING THE INTERLAYER MICROPORES

The microporous clay minerals can be modified in three main ways :

- By altering the anionic layer charge and hence the concentration of interlayer cations.
- By altering the charge on the interlayer cations and therefore their number.
- By varying the size and shape of the cations.

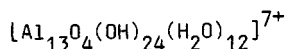
An example of each of these three methods follows. The effect of layer charge is seen in Table 5 for  $\text{Co}^{\text{III}}(\text{en})_3\text{-FH90}$  and  $\text{Co}^{\text{III}}(\text{en})_3\text{-FH150}$ , and is due to changes in the free distance  $d_3$  between adjacent pairs of cations.  $d_3$  was estimated as 6.7 and 3.4 Å respectively, whereas the vertical free distance between siliceous layers was 4.2 Å for each sorbent. As a result the  $\text{Co}^{\text{III}}(\text{en})_3\text{-FH90}$  intercalated molecules as large as neo-pentane whereas in  $\text{Co}^{\text{III}}(\text{en})_3\text{-FH150}$  at 77.3K  $\text{O}_2$  was intercalated but  $\text{N}_2$  was not.

The effect of charge on the cation is seen among the alkylammonium and alkyldiammonium cations of Table 4. The ions  $\text{CH}_3\text{CH}_2\text{CH}_2\text{NH}_3^+$  and  $\text{NH}_3^+\text{CH}_2\text{CH}_2\text{NH}_3^+$  have about the same length and volume, but only half the number of the divalent ions is required as compared with the monovalent ones. This increased the distance  $d_3$  and gave more open space between cations, as reflected in the interlayer free areas of 278 and 184  $\text{m}^2\text{g}^{-1}$ .

The effect of shape and size of cations is illustrated by comparing  $\text{CH}_3\text{NH}_3^-$  and  $(\text{CH}_3)_4\text{N}^-$ -montmorillonites, having  $d_1$  equal to 2.2 and 4.1 Å respectively. At 323K the  $\text{CH}_3\text{NH}_3^-$  form did not intercalate iso- $\text{C}_5\text{H}_{12}$ , iso- $\text{C}_8\text{H}_{16}$  or cyclohexane appreciably, whereas all these molecules were intercalated by the  $(\text{CH}_3)_4\text{N}^-$ -montmorillonite. A large increase in  $d_1$  would be needed to intercalate these hydrocarbons in  $\text{CH}_3\text{NH}_3^-$ -montmorillonite, with threshold pressures for intercalation which were not reached in our conditions. For  $(\text{CH}_3)_4\text{N}^-$ -montmorillonite the increase needed in  $d_1$  is much less and intercalation proceeded ( $\Delta G$  in eqn. 2 is negative).

## 9. MICROPOROUS PILLARED CLAY MINERALS

Attention is increasingly being directed towards replacements of interlayer cations ( $\text{Na}^+$ ,  $\text{Ca}^{2+}$  etc) (in montmorillonites, beidellite, nontronite, hectorites, fluorhectorites, rectorite and tetrasilicic micas) by oligomeric cations of elements such as Al, Zr, Ti, Cr and Fe. An example of such a cation is the Keggin ion



found in aluminium chlorhydrol solutions. The objectives have been to increase the interlayer free distances,  $d_1$ , and, by replacing organic ions by inorganic ones, to improve the thermal and hydrothermal stabilities of the products. In this way it is hoped to obtain good microporous catalysts more open than zeolites and of high surface area, for dewaxing, hydrocracking, and cracking of heavy oil fractions and biomass oils.

Table 6 gives examples of reported results for interlayer free distances and for monolayer equivalent areas in some studies on pillared clays (PILCS).

The distances  $d_1$  have been successfully increased, as were the thermal and hydrothermal stabilities, when compared with those of the microporous organoclays. The BET monolayer equivalent areas also show increases relative to the organoclays in some but not all the products. The value of  $d_1$  after calcination is a function of the method of preparation, the calcination temperatures and the type of layer silicate and oligomeric oxyanion.

TABLE 6. Interlayer free distances,  $d_1 = d(001) - 9.4$ , in Å, and monolayer equivalent areas (MEA) in  $\text{m}^2\text{g}^{-1}$  in some PILCS.

Pillar based on:	Pillaring via:	After Calcination: $d_1$	MEA	Reference
Al	Oligomeric cations	8.4-91	~400	19,20
Al	" "	6.8	300	21
(Si, Al)	" "	6.0-10.2	85-430	22
(Si, Al)	" "	6.6-8.8	340-500	22
Si	$[\text{Si}(\text{acetylacetonate})_3]^+$	3.2(max.)	40-190	23
Si	Silsesquioxanes	6.8-10.4	140-400	24
Zr	Oligomeric cations	8.6	260	19
Zr	" "	12.4	290	19
Zr	" "	12.4 & 16.2	250	19
Ti	" "	15.6	300	25
Ti	" "	19.4	330	25
Cr	" "	11.6	430	26
Fe	$[\text{Fe}_3(\text{OCOCH}_3)_7\text{OH}]^+$	7.3	280	27

The free distances,  $d_3$ , between adjacent pillars are, however, not well defined. One ideal model assumes the pillars to be equally spaced, but there is not yet much supporting evidence. It seems more probable that in calcination some pillars may fuse together, giving a range in values of  $d_3$ . If this is the case the micropores will be more irregular than those in the organoclay molecular sieves and in zeolites. Isotherms are of types 1 or 2 and some give evidence of mesoporosity, as estimated from  $\text{N}_2$  desorption.

## 10. CONCLUDING REMARKS

It is hoped that enough has been said to clarify the diversity of behaviour found among sorbents based on layer silicates. Much remains to be explored in all areas, and especially in the fast expanding chemistry of PILC's. In this latter area more knowledge is needed about the extent and origin of mesoporosity and the degree of regularity in micropore dimensions, and also about the nature of the pillars after and before calcination, the ways in which they are attached to the siliceous layers and how they may be chemically modified to improve catalytic properties. More knowledge is also required about the chemical species present in pillaring solutions.

## REFERENCES

1. K. Brauner and A. Preisinger, *Tschermak's mineral. u. petrog. Mitt.*, 1956, 6, 120.
2. A. Weiss, *Chem. Ber.*, 1958, 91, 487.
3. R.M. Barrer and D.M. MacLeod, *Trans. Faraday Soc.*, 1954, 50, 980.
4. R.M. Barrer and N. Mackenzie, *J. Phys. Chem.*, 1954, 58, 560.
5. S. Brunauer, "The Adsorption of Gases and Vapours" (Oxford Univ. Press), 1944, p. 150.
6. R.M. Barrer, N. Mackenzie and A.D. MacLeod, *J. Phys. Chem.*, 1954, 58, 568.
7. A. Preisinger, *Clays and Clay Minerals*, 1957, 6, 61.
8. R.M. Barrer, *Phil. Trans. R. Soc. Lond.*, 1984, A 311, 333.
9. S.A. Allison and R.M. Barrer, *Trans. Faraday Soc.*, 1968, 64, 549.
10. R.M. Barrer and K.E. Kelsey, *Trans. Faraday Soc.*, 1961, 57, 625.
11. R.M. Barrer, *J. of Inclusion Phenomena*, 1986, 4, 109.
12. R.M. Barrer and D.M. MacLeod, *Trans. Faraday Soc.*, 1955, 51, 1290.
13. R.M. Barrer and A.D. Millington, *J. of Colloid and Interface Science*, 1967, 25, 359.
14. R.M. Barrer and D.L. Jones, *J. Chem. Soc. A*, 1970, 1531.
15. R.M. Barrer and D.L. Jones, *J. Chem. Soc. A*, 1971, 2594.
16. R.M. Barrer and G.S. Perry, *J. Chem. Soc.*, 1961, 842.
17. R.M. Barrer and G.S. Perry, *J. Chem. Soc.*, 1961, 850.
18. R.M. Barrer and M.G. Hampton, *Trans. Faraday Soc.*, 1957, 53, 1462.
19. D.E.W. Vaughan, R.J. Lussier and J.S. Magee, 1979, U.S.P. 4,176,090.
20. D.E.W. Vaughan and R.J. Lussier, in "Proc, 5<sup>th</sup> Int. Conference on Zeolites", Ed. L.V.C. Rees, (Heyden), 1980 p. 94.
21. A. Schutz, W.E.E. Stone, G. Poncelet and J.J. Fripiat, *Clays and Clay Minerals*, 1987, 35, 251.
22. J. Sterte and J. Shabtai, *Clays and Clay Minerals*, 1987, 35, 429.
23. T. Endo, M.M. Mortland and T.J. Pinnavaia, *Clays and Clay Minerals*, 1980, 28, 105.
24. R.M. Lewis, K.C. Ott and R.A. Van Santen, 1985, U.S.P. 4,510,257.
25. J. Sterte, *Clays and Clay Minerals*, 1986, 34, 658.
26. T.J. Pinnavaia, M.S. Tsou and S.D. Landau, *J. Amer. Chem. Soc.*, 1985, 107, 4783.
27. S. Yamanaka, T. Doi, S. Sako and M. Hattori, *Mat. Res. Bull.*, 1984, 19, 161.